THEMIS observations of penetration of the plasma sheet into the ring current region during a magnetic storm

Chih-Ping Wang,[1] Larry R. Lyons,[1] Vassilis Angelopoulos,[2] Davin Larson,[3] J. P. McFadden,[3] Sabine Frey,[3] Hans-Ulrich Auster,[4] and Werner Magnes[5]

[1] Observations from the THEMIS spacecraft during a weak magnetic storm clearly show that the inner edge of the ion plasma sheet near dusk moved from $r \sim 6\ R_E$ during the pre-storm quiet time to $r \sim 3.5\ R_E$ during the main phase, and then moved outward during the recovery phase. The plasma sheet particles from the tail reached the inner magnetosphere during the main phase through open drift paths, which extended earthward with increasing convection, and were energized to ring current energies, resulting in an increase in ring current population. During the recovery phase, the plasma sheet region retreated to outside the inner magnetosphere as the region of open drift paths moved outward with decreasing convection, leaving the ring current particles within the expended closed drift path region. With no new particles from the plasma sheet, ring current population gradually decreased due to losses as the recovery phase proceeded. **Citation:** Wang, C.-P., L. R. Lyons, V. Angelopoulos, D. Larson, J. P. McFadden, S. Frey, H.-U. Auster, and W. Magnes (2008), THEMIS observations of penetration of the plasma sheet into the ring current region during a magnetic storm, *Geophys. Res. Lett.*, *35*, L17S14, doi:10.1029/2008GL033375.

1. Introduction

[2] Plasma sheet particles, which originally come from the solar wind and ionosphere and are within the region of open electric and magnetic drift paths, have been assumed to be the major particle source for the ring current population (10 – 200 keV ions and electrons) in particle simulations for the ring current [e.g., *Chen et al.*, 2006]. According to the models, the inner edge of the plasma sheet (the separatrix between the regions of open and closed particle drift paths) should move earthward when the convection electric field is enhanced, such as during a storm main phase, thus allowing the particles from the tail plasma sheet to have access to the inner magnetosphere and to be adiabatically energized to the ring current energy range. Once inside the inner magnetosphere, higher energy particles can be further energized by radial and energy diffusion, but it is the earthward movement and adiabatic energization of plasma sheet particles that is critical to ring current enhancement within the models. The CRRES Observations in the region of $r < \sim 5.3\ R_E$ [*Korth et al.*, 2000] have supported the above hypothesis, but didn't directly identify the ring current population as plasma sheet particles.

[3] The inbound passes of the THEMIS spacecraft from $r \sim 15$ to $\sim 2\ R_E$ at the same near-dusk local times during different phases of a weak storm in May, 2007 (minimum Dst $= -60$ nT on May 23, which is the strongest storm in 2007 since the THEMIS spacecraft began operations in March 2007) provide unprecedented end to end measurements of the equatorial plasma sheet from its outward boundary at the magnetopause, to its earthward boundary, and into the ring current region, which allows us to obtain an unambiguous determination of the radial extent of the plasma sheet and its variation throughout the storm. The THEMIS results clearly show that the plasma sheet penetrated earthward into the inner magnetosphere during the storm main phase and plasma sheet particles were energized to the ring current energy range, resulting in an increase in the number of ring current particles. This clearly indicates that the majority of the ring current particles were originally plasma sheet particles that have access to the inner magnetosphere along the open drift paths, as assumed in the models.

2. THEMIS Observations During the Storm

[4] The THEMIS mission consists of five spacecraft orbiting near the equatorial plane [*Angelopoulos*, 2008]. The ions and electrons are measured by an electrostatic analyzer (ESA, $0.006 – 20$ keV/q for ions and $0.007 – 26$ keV for electrons [*McFadden et al.*, 2008]) and a solid state telescope (SST, ~ 28 keV – 6 MeV for ions and electrons (*D. Larson et al.*, Solid state telescope for THEMIS, submitted to *Space Science Reviews*, 2008)). The magnetic field (3 seconds average of spin fitted data) is measured by the FGM instrument [*Auster et al.*, 2008]. The Dst and the interplanetary conditions from Wind for the storm are shown in Figures 1a to 1c. Throughout the storm, the multiple THEMIS spacecraft were lined up and passed through nearly the same locations about once per day. The trajectories of the THEMIS spacecraft (moving toward smaller radial distance) during five different phases (pre-storm quiet time, sudden commencement, main phase, early recovery, and late recovery) are shown in Figure 1d. For the five phases, we used data from THEMIS B, E, D, D, B, respectively for the best data coverage and quality. The

---
[1]Department of Atmospheric and Oceanic Sciences, University of California, Los Angeles, California, USA.
[2]Department of Earth and Space Sciences, University of California, Los Angeles, California, USA.
[3]Space Sciences Laboratory, University of California, Berkeley, California, USA.
[4]Institut für Geophysik und Extraterrestrische Physik, Technische Universität Braunschweig, Braunschweig, Germany.
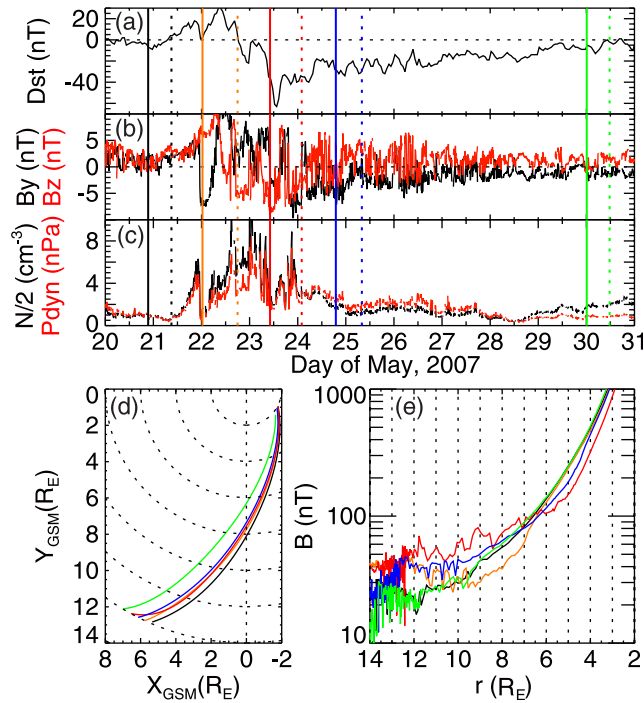[5]Space Research Institute, Austrian Academy of Sciences, Graz, Austria.

Figure 1. (a) Dst, (b) the IMF By and Bz (GSM), and (c) 0.5×solar wind density, and solar wind dynamic pressure measured by WIND (time shifted to the bowshock nose) during the May 2007 storm. The vertical lines indicate the five phases of the storm (solid (dashed): THEMIS passed $r = 14$ (2) R_E; black: pre-storm quiet time, orange: sudden commencement, red: main phase, blue: early recovery, green: late recovery, the same color coding is used for Figures 1d and 1e). (d) Trajectories of the THEMIS spacecraft. (e) Magnetic field strengths as a function of radial distance.

magnetic field strengths as a function of radial distance r are shown in Figure 1e, and it can be seen that the magnetic fields in the inner magnetosphere ($r < 6\ R_E$) became weaker during the main phase due to the enhanced ring current. (r is computed from the projection of the spacecraft positions unto the X-Y GSM plane. The Z_{GSM} of the spacecraft is < ~2 R_E and is smaller closer to the Earth.)

[5] We define the ring current population as ions and electrons of energy from 30 to 200 keV in the region between $r = 2$ and 7 R_E. Figure 2 shows the spectra of omnidirectional energy fluxes as a function of r during the five different phases of the storm. During the pre-storm quiet time, it can be seen from Figure 2a that the energy fluxes changed sharply at $r \sim 13.7\ R_E$ in both ions and electrons as the spacecraft moved across the magnetopause from the colder magnetosheath to the hotter magnetosphere. Inside the magnetosphere, the spacecraft continuously observed similar magnitudes of ion energy fluxes peaking at ~20 keV as it moved earthward to $r \sim 8\ R_E$. Within the ring current region, the peak of ion energy fluxes increased with decreasing r. The very uniform fluxes below ~30 keV seen in ions and electrons at all times by the ESA in the region between ~3 to 7 R_E are due to data contamination by penetrating energetic electrons. The contamination becomes very strong after the storm main phase. Since we only

consider >30 keV ring current particles, this contamination does not affect our results. For the electrons inside the magnetosphere, energy fluxes peaking at ~7 keV are seen continuously only to $r \sim 12\ R_E$ and then decrease significantly. Within the ring current, the energy fluxes are higher at $r \sim 5{-}7\ R_E$ and $r < 3\ R_E$, which are the outer and inner electron radiation belts.

[6] Figure 3 shows phase space densities (f) multiplied by μ as a function of μ versus r (we take $\mu = E_k/B$ and show it in units of keV/5 nT, where E_k is particle's kinetic energy, B is local magnetic field strength as shown in Figure 1e, and 5 nT was chosen as a typical equatorial magnetic field strength in the tail plasma sheet. f is computed using the omnidirectional fluxes shown in Figure 2. We plot μf instead of f because it is easier to discern the radial variations of μf at different μ from the color contours than for f.) The lower and higher dashed curves indicate the μ values that correspond to $E_k = 30$ keV and 200 keV, respectively, that we selected for the ring current energy range. As shown in Figure 3a, during the quiet time, f at μ values typical for the plasma sheet particles ($\mu \sim 1$ to 10 keV/5 nT for ions and $\mu \sim 0.1$ to 2 keV/5 nT for electrons) is seen to have similar values in the region from the magnetopause to $r \sim 6{-}8\ R_E$ for ions and $r \sim 11.5{-}12\ R_E$ for electrons, and then drop quickly. The sharp drop is
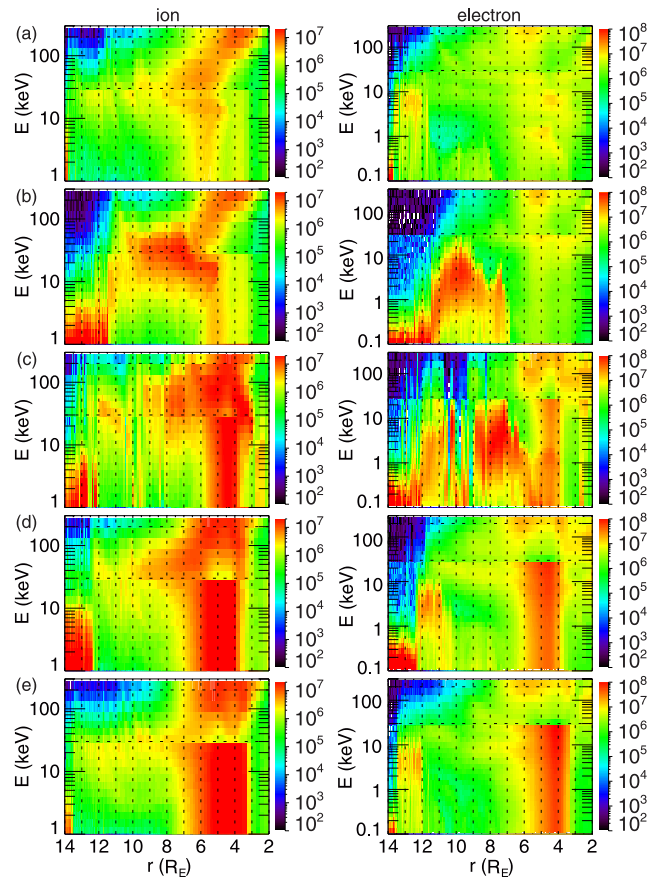

Figure 2. Energy flux (color bar unit keV/s · sr · cm^2 · keV) vs. energy as a function of radial distance for ions (left) and electrons (right) for (a) pre-storm, (b) sudden commencement, (c) main phase, (d) early recovery, and (e) late recovery.
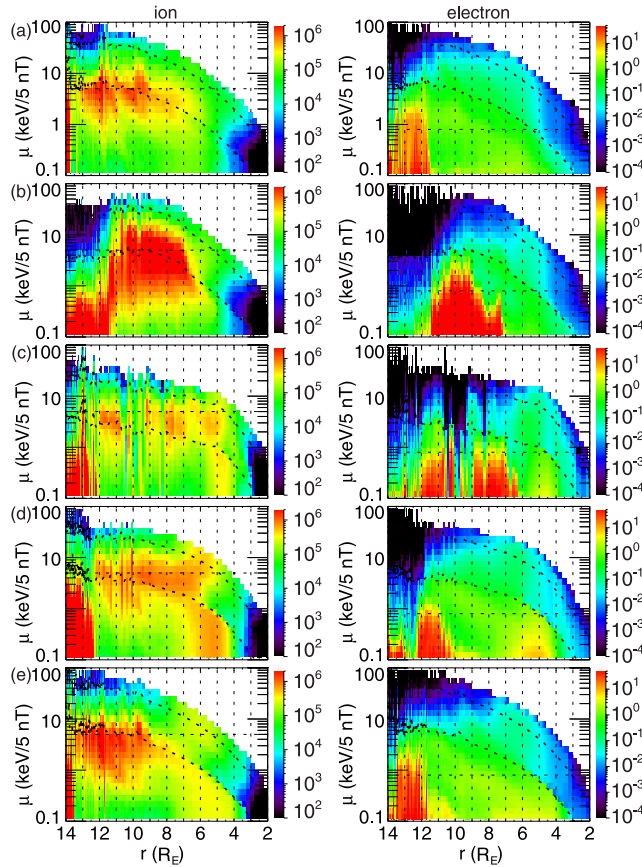
Figure 3. $f\mu$ (color bar unit $s^3 \cdot km^{-6} \cdot keV/5\ nT$) vs. μ as a function of radial distance for ions (left) and electrons (right) for (a) pre-storm, (b) sudden commencement, (c) main phase, (d) early recovery, and (e) late recovery. The lower and upper dashed curves indicate $E_K = 30$ and 200 keV, respectively.

energy dispersive with f of higher μ decreasing at larger r. This is consistent with the energy-dependent separatrix between open and closed particle drift paths (the Alfvén layers), indicating the drops are the inner edges of the plasma sheet. The similar phase space densities seen in the region between the magnetopause and the inner edges indicate that the populations within this region are plasma sheet particles coming from the tail along open drift paths.

[7] As shown in Figure 3, the μ values for the two constant E_k curves decrease substantially with decreasing r because of the increasing B. Thus ring current ions (electrons) inside $r \sim 6$ (4) R_E have the same μ values as do the particles in the plasma sheet, indicating that the plasma sheet ions that have a typical energy of ~ 5 keV in the tail would be energized to ring current energies if their open drift paths extend to the inner magnetosphere. However, during the pre-storm quiet time, the locations of the plasma sheet inner edges clearly show that the open drift paths for both ions and electrons did not extend to the ring current region so that the quiet-time ring current populations were not plasma sheet particles within the open drift path region.

[8] As shown in Figures 2b and 3b, during the storm sudden commencement resulting from a solar wind dynamic

pressure enhancement (mainly due to an increase in the solar wind density), the magnetopause was pushed earthward to $r \sim 11.5\ R_E$ and the inner edges of the plasma sheet also moved earthward (to $\sim 5-6\ R_E$ for ions and $\sim 7-7.5\ R_E$ for electrons). The energy fluxes and f in the plasma sheet are seen to have become much higher than during the quiet time pass, while those in the ring current did not change significantly. The enhancement within the plasma sheet is likely due to the higher solar wind density (average solar wind density was 8.9 cm^{-3} during the sudden commencement period compared to 1.4 cm^{-3} during the preceding quiet time period) providing more source particles for the plasma sheet. Since most of the ring current region was still earthward of the inner edges of the plasma sheet and thus remained within the closed drift path region, the energy fluxes and f in the ring current did not change in response to the increase in the solar wind density.

[9] During the storm main phase (Figures 2c and 3c), the energy fluxes of ring current ions and electrons are seen to be much higher than those during the previous two phases. Also, the peak energy of the plasma sheet fluxes became higher, indicating the plasma sheet temperature increased. The f show that the plasma sheet extended further earthward (to $\sim 3.5-4.5\ R_E$ for ions and $\sim 6-7\ R_E$ for electrons), and that the substantial increases in f within the ring current region were at plasma sheet μ values and within the portion of the plasma sheet that penetrated earthward. This clearly indicates that, during the main phase when convection was strong, the ions' open drift paths extended earthward and well into the ring current region and it is the addition of particles coming from the tail plasma sheet that leads to the increase in the ring current population, and thus the enhanced ring current ion energy fluxes. There is also a clear increase in the electron f in the ring current, however, the electron plasma sheet is seen to only have extended to $r \sim 6\ R_E$ at dusk local times. However, as discussed later, the electron inner edge is expected to be much closer to the Earth at dawn than at dusk as shown in Figure 4, suggesting that the THEMIS spacecraft was not at the right local times to directly observe plasma sheet electrons penetrating well into the ring current region. Therefore, it is likely that the
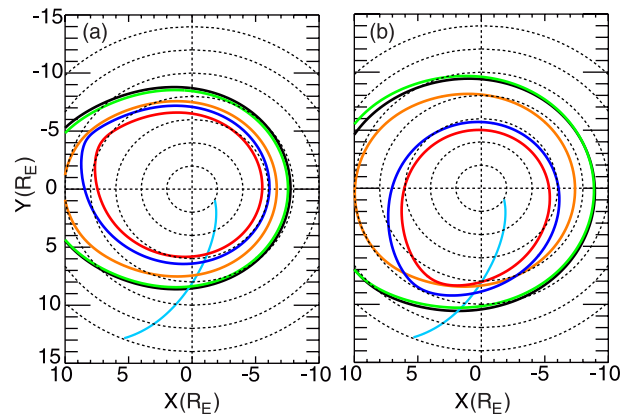

Figure 4. (a) Drift separatrix for ions of $\mu = 5$ keV/5 nT and (b) electrons of $\mu = 0.8$ keV/5 nT during the five storm phases (the same color coding as Figure 1a). The blue curve indicates the spacecraft trajectory.

electron increase inside $r = 6$ R_E is due to electrons having penetrated to $r < 6$ R_E at post-midnight local times and then drifting eastward to the dusk region. The lower-energy electrons are also expected to undergo strong losses [e.g., *Chen et al.*, 2006], which would reduce their phase space densities relative to those within the plasma sheet by the time they reach dusk local times, consistent with the observations. Also, other local energization processes can enhance the fluxes of higher-energy electrons in addition to the drift associated adiabatic energization [e.g., *Chen et al.*, 2006].

[10] During the early recovery phase (Figures 2d and 3d), the energy fluxes in the ring current decreased from their main phase values but remained higher than their quiet time values. The *f* show that the inner edge of electron plasma sheet moved outward to $10-11$ R_E, so that ring current electrons were left within the closed drift path region. The electron *f* within the closed drift path region was significantly lower than that during the main phase but is still higher than that during the quiet time, indicating strong losses. For ions, *f* at $\mu < \sim 3$ keV/5 nT is seen to drop at $r \sim 6$ R_E but *f* at $\mu > \sim 3$ keV/5 nT is seen to drop at $r \sim 5$ R_E, which is opposite to the inner edge energy dispersion seen in the previous storm phases and is likely a result of energy-dependent losses. The closed drift path region had only recently expanded over ion ring current this early during the recovery phase, and losses are stronger for lower energy ions than for higher energy ions (at $L = 5$, the lifetime for 30 keV proton is ~ 1 day while for 200 keV proton it is ~ 10 days [*Fok et al.*, 1991]). Because of this, *f* at higher μ is not expected to be very different from its values during the main phase, but *f* at lower μ can be substantially lower than its main phase values. We thus expect that the outward motion of open drift paths is better indicated by *f* at lower μ than *f* at lower μ.

[11] During the late recovery phase (Figures 2e and 3e), the energy fluxes in the ion and electron plasma sheet were almost the same as those of the pre-storm quiet time. However, the energy fluxes in the ring current were still higher than their quiet time values. The *f* clearly show that the inner edges of the ion and electron plasma sheet moved further outward and back to their quiet time locations, and a clear separation developed between the region of plasma sheet ions moving along open drift paths and the ions that were previously plasma sheet ions and were now left within the closed drift path region. The *f* in the ring current was lower than that during the main phase due to loss but it remained clearly higher than its pre-storm quiet time value.

[12] The above storm sequence clearly shows that during the main phase the majority of the ring current ions are plasma sheet particles moving along open drift paths from the tail source, as assumed in particle simulations for the ring current.

[13] As a test of the inferences described above, we compare the observed inner edges with a simple model prediction of the drift separatrix. Figure 4 shows the drift separatrix for protons (electrons) of $\mu = 5$ (0.8) keV/5 nT obtained from contours of constant $\mu B + q\Phi$, where q is electric charge (positive for protons and negative for electrons). B is the equatorial magnetic field strength obtained from the Tsyganenko 96 magnetic field model (T96) [*Tsyganenko*, 1996], and Φ is the electric field potential

including corotation and convection obtained from the Volland-Stern model [*Volland*, 1973; *Stern*, 1974], $\Phi(r, \phi) = -V_\Omega/r + V_0/2(r/r^*)^a \sin\phi$, where $V_\Omega = 90$ kV, r is radial distance, ϕ is local time, and higher a gives stronger shielding of the convection electric field in the inner magnetosphere ($a = 1.5$ for the quiet time, sudden commencement, and late recovery phase, and $a = 0.5$ for the main phase and the early recovery phase). We choose $r^* = 60$ R_E. The interplanetary conditions and Dst averaged within the time period of each phase are used for T96 and for computing V_0 according to *Siscoe et al.* [2002]. As shown in Figure 4, the plasma sheet ions can go further earthward than do the plasma sheet electrons at dusk local times, as observed by the THEMIS spacecraft. Plasma sheet electrons can penetrate much further earthward at dawn than at dusk local times under strong convection, suggesting why the THEMIS spacecraft did not observe plasma sheet electrons extending well into the inner magnetosphere during the main phase. The locations of the inner edges from the observations/model during the five phases for ions (electrons) are, quiet time: 9/8.6 (10.6/10.7), sudden commencement: 7/7.5 (9/8.5), main phase: 4.5/5.7 (7/8.2), early recovery: 5.2/6.5 (11/9.2), late recovery: 9/8.5 (12/10.7). Considering these are steady separatrix locations predicted using averaged interplanetary conditions, the comparisons show that the inward and outward motions of the inner edges during different phases of a storm and the difference in the ion and electron inner edge agree reasonably well with the expectations from the drift physics included in the simple model. More realistic modeling is beyond the scope of this study.

3. Conclusions

[14] The THEMIIS observations of the radial extent of the plasma sheet at fixed local times near dusk during a weak storm clearly show that the ring current ions during the main phase are plasma sheet ions moving along open drift paths when enhanced convection moves the inner edge of the ion plasma sheet earthward to the inner magnetosphere. During the ensuing recovery phase, the inner edge of the plasma sheet moved out of the inner magnetosphere with decreasing convection strength, leaving the ring current particles injected during the main phase within the closed drift path region. With no particle addition from the plasma sheet, the ring current decayed due to loss processes. The observed locations and variations of the inner edges of the plasma sheet throughout the storm agree reasonably well with the model predicted drift separatrix locations. These observations therefore confirm the drift physics used in ring current particle simulations and their assumption that plasma sheet particles are the major source particles for the ring current population. The observed changes in the inner edge of the electron plasma sheet indicate that the same drift physics should account for the changes in the electron ring current, but the THEMIS spacecraft were not at dawnside local times where earthward penetration of the electron plasma sheet deep into the inner magnetosphere is expected to be observed, but did see these electrons following their azimuthal drift to the duskside.

References

Angelopoulos, V. (2008), The THEMIS mission, *Space Sci. Rev.*, in press.

Auster, H. U., et al. (2008), The THEMIS fluxgate magnetometer, *Space Sci. Rev*, in press.

Chen, M. W., S. Liu, M. Schulz, J. L. Roeder, and L. R. Lyons (2006), Magnetically self-consistent ring current simulations during the 19 October 1998 storm, *J. Geophys. Res.*, *111*, A11S15, doi:10.1029/2006JA011620.

Fok, M.-C., J. U. Kozyra, A. F. Nagy, and T. E. Cravens (1991), Lifetime of ring current particles due to Coulomb collisions in the plasmasphere, *J. Geophys. Res.*, *96*(A5), 7861–7868.

Korth, A., R. H. W. Friedel, C. G. Mouikis, J. F. Fennell, J. R. Wygant, and H. Korth (2000), Comprehensive particle and field observations of magnetic storms at different local times from the CRRES spacecraft, *J. Geophys. Res.*, *105*(A8), 18,729–18,740.

McFadden, J. P., C. W. Carlson, D. Larson, V. Angelopolos, M. Ludlam, R. Abiad, and B. Elliot (2008), The THEMIS ESA plasma instrument and in-flight calibration, *Space Sci. Rev*, in press.

Siscoe, G. L., G. M. Erickson, B. U. Ö. Sonnerup, N. C. Maynard, J. A. Schoendorf, K. D. Siebert, D. R. Weimer, W. W. White, and G. R. Wilson (2002), Hill model of transpolar potential saturation: Comparisons with MHD simulations, *J. Geophys. Res.*, *107*(A6), 1075, doi:10.1029/2001JA000109.

Stern, D. (1974), Models of the Earth's electric field, *Rep. X-602-74-159*, NASA Goddard Space Flight Cent., Greenbelt, Md.

Tsyganenko, N. A. (1996), Effects of the solar wind conditions on the global magnetospheric configuration as deduced from data-based field models, in *Proceedings of the ICS-3 Conference on Substorms*, edited by E. J. Rolfe and B. Kaldeich, *Eur. Space Agency Spec. Publ., ESA SP*, *389*, 181–185.

Volland, H. (1973), A semiempirical model of large-scale magnetospheric electric fields, *J. Geophys. Res.*, *78*(1), 171–180.

———————————

V. Angelopoulos, Department of Earth and Space Sciences, University of California, Los Angeles, CA 90095-1567, USA.

H.-U. Auster, Institut für Geophysik und Extraterrestrische Physik, Technische Universität Braunschweig, D-38106 Braunschweig, Germany.

S. Frey, D. Larson, and J. P. McFadden, Space Sciences Laboratory, University of California, Berkeley, CA 94720, USA.

L. R. Lyons and C.-P. Wang, Department of Atmospheric and Oceanic Sciences, University of California, Los Angeles, CA 90095-1565, USA. (cat@atmos.ucla.edu)

W. Magnes, Space Research Institute, Austrian Academy of Sciences, A-8042 Graz, Austria.